RESEARCH ARTICLE

# N-Acylethanolamine acid amidase (NAAA) is dysregulated in colorectal cancer patients and its inhibition reduces experimental cancer growth

Barbara Romano[1,2] | Ester Pagano[1,2] | Fabio A. Iannotti[2,3] |
Fabiana Piscitelli[2,3] | Vincenzo Brancaleone[4] | Giuseppe Lucariello[1] |
Maria Francesca Nani[1,2] | Ferdinando Fiorino[1] | Rosa Sparaco[1] |
Giovanna Vanacore[1] | Federica Di Tella[1] | Donatella Cicia[1] | Ruggero Lionetti[5] |
Alexandros Makriyannis[6] | Michael Malamas[6] | Marcello De Luca[5] |
Giovanni Aprea[7] | Maria D'Armiento[8] | Raffaele Capasso[2,9] | Bernardo Sbarro[1] |
Tommaso Venneri[1,2] | Vincenzo Di Marzo[2,3,10,11] | Francesca Borrelli[1,2] |
Angelo A. Izzo[1,2]

[1]Department of Pharmacy, School of Medicine and Surgery, University of Naples Federico II, Naples, Italy

[2]Endocannabinoid Research Group, Pozzuoli, Italy

[3]Institute of Biomolecular Chemistry, Consiglio Nazionale delle Ricerche, Pozzuoli, Italy

[4]Department of Science, University of Basilicata, Potenza, Italy

[5]Department of Public Health, School of Medicine and Surgery, University of Naples Federico II, Naples, Italy

[6]Center for Drug Discovery and Departments of Chemistry and Chemical Biology and Pharmaceutical Sciences, Northeastern University, Boston, Massachusetts, USA

[7]Department of Clinical Medicine and Surgery, Interuniversity Center for Technological Innovation Interdepartmental Center for Robotic Surgery, University of Naples Federico II, Naples, Italy

[8]Department of Biomorphological and Functional Science, School of Medicine and Surgery, University of Naples Federico II, Naples, Italy

[9]Department of Agricultural Sciences, University of Naples Federico II, Naples, Italy

[10]Centre de Recherche de l'Institut Universitaire de Cardiologie et Pneumologie de Quèbec, Quebec City, Quebec, Canada

[11]Institut sur la Nutrition et les Aliments Fonctionnels, Université Laval, Quebec City, Quebec, Canada

Correspondence
Francesca Borrelli, Department of Pharmacy, School of Medicine and Surgery, University of Naples Federico II, Naples, Italy.
Email: franborr@unina.it

**Background and Purpose:** N-Acylethanolamine acid amidase (NAAA) is a lysosomal enzyme accountable for the breakdown of N-acylethanolamines (NAEs) and its pharmacological inhibition has beneficial effects in inflammatory conditions. The

knowledge of NAAA in cancer is fragmentary with an unclarified mechanism, whereas its contribution to colorectal cancer (CRC) is unknown to date.

**Experimental Approach:** CRC xenograft and azoxymethane models were used to assess the in vivo effect of NAAA inhibition. Further, the tumour secretome was evaluated by an oncogenic array, CRC cell lines were used for in vitro studies, cell cycle was analysed by cytofluorimetry, NAAA was knocked down with siRNA, human biopsies were obtained from surgically resected CRC patients, gene expression was measured by RT-PCR and NAEs were measured by LC–MS.

**Key Results:** The NAAA inhibitor AM9053 reduced CRC xenograft tumour growth and counteracted tumour development in the azoxymethane model. NAAA inhibition affected the composition of the tumour secretome inhibiting the expression of EGF family members. In CRC cells, AM9053 reduced proliferation with a mechanism mediated by PPAR-α and TRPV1. AM9053 induced cell cycle arrest in the S phase associated with cyclin A2/CDK2 down-regulation. NAAA knock-down mirrored the effects of NAAA inhibition with AM9053. NAAA expression was down-regulated in human CRC tissues, with a consequential augmentation of NAE levels and dysregulation of some of their targets.

**Conclusion and Implications:** Our results show novel data on the functional importance of NAAA in CRC progression and the mechanism involved. We propose that this enzyme is a valid drug target for the treatment of CRC growth and development.

**KEYWORDS**
acylethanolamides, colon cancer, endocannabinoid system

# 1 | INTRODUCTION

Colorectal cancer (CRC) is a predominant healthcare problem in Europe (Malvezzi et al., 2019) and accounts to become the third leading cause of predicted cancer deaths in the United States (Siegel et al., 2021) for the year 2021. Notwithstanding the significant strides that have been made in CRC treatment, the 5-year survival rate of patients suffering from the late stages of the disease remains still around 12% (Kalyan et al., 2018). Further research leading to the discovery of new effective drugs is vital to provide new therapeutic opportunities to reduce the burden of the disease. There is a wealth of preclinical data providing evidence that endogenous lipids may differently affect one or more hallmarks of cancer (Pisanti et al., 2013), thus representing one of the most promising therapeutic areas.

N-Acylethanolamines (NAEs), such as **N-palmitoylethanolamine (PEA)**, **anandamide (N-arachidonoylethanolamine, AEA)** and **N-oleoylethanolamine (OEA)**, are endogenous bioactive lipids that affect a plethora of physiological functions including pain, inflammation, anxiety, cognition and food intake (Bottemanne et al., 2018). Their functional role in CRC is an object of debate, anandamide is well established (Ligresti et al., 2003), PEA's are still being investigated, while OEA's are only at the very beginning. Further, there is little knowledge about the effects and/or mechanism of action of the latter two biolipids (Grill et al., 2019). Two enzymes are believed to be

### What is already known

- Treatment of colon cancer remains a significant unmet need.
- Little is known about the role of N-acylethanolamine acid amidase (NAAA) in cancer and the possible mechanisms.

### What does this study add

- This study provides novel evidence on the involvement of NAAA in colon carcinogenesis.

### What is the clinical significance

- NAAA inhibitors may represent a novel pharmacological opportunity to counteract colorectal cancer growth and development.

involved in NAE hydrolysis and, therefore, regulation of NAE endogenous levels are **fatty acid amide hydrolase (FAAH)** and **N-acylethanolamine acid amidase (NAAA)** (Bottemanne et al., 2018).

The role of FAAH in CRC is well recognized, its pharmacological inhibition resulting in beneficial effects due to the enhancement of anandamide levels (Izzo et al., 2008; Ligresti et al., 2003). Based on this finding, inhibition of NAE hydrolytic enzymes represents a major area of interest.

NAAA is an N-terminal cysteine hydrolase of the choloylglycine hydrolase family, mainly localized in lysosomes (Tsuboi et al., 2005; Tsuboi et al., 2007). NAAA has been reported to be expressed in immune cells (Su et al., 2004), but it is also found in the prostate and lung epithelium (Su et al., 2004; Wang et al., 2008), as well as in small and large intestine (Alhouayek et al., 2015; Borrelli et al., 2015).

Over the last decade, several NAAA inhibitors have been developed in order to take advantage of the beneficial effects derived from the pharmacologically induced increase of NAE tissue levels and also to improve our knowledge of the pathophysiological role of this enzyme (Bottemanne et al., 2018). NAAA inhibitors have been primarily studied in the context of inflammation, immune disorders and pain (Bottemanne et al., 2018). However, our knowledge of the function of NAAA in cancer is largely fragmentary, with only a few reports hypothesizing its potential role in prostate and ovarian carcinogenesis, via a yet unclarified mechanism (Du et al., 2016; Liu et al., 2014; Sakura et al., 2016; Wang et al., 2008). In this respect, the pathophysiological role of NAAA in CRC is unknown, with no published reports to date. Therefore our study was aimed at elucidating, for the first time, the role of NAAA in CRC, through the assessment of the effects of the selective NAAA inhibitor AM9053 on CRC growth in vivo and in vitro, along with the analysis of the proliferative behaviour of a CRC cell line genetically silenced for NAAA. Finally, the evaluation of NAAA expression in human CRC tissues.

## 2 | METHODS

### 2.1 | Patient samples

Primary tumoural colon biopsies were obtained from surgical specimens of $n = 19$ patients, admitted for colon resection due to a CRC diagnosis, with different tumour–node–metastasis (TNM) stage, ranging from T2 to T4 (pT2 [$n = 6$], pT3 [$n = 7$] and pT4 [$n = 6$]). The areas of the intestinal mucosa, defined as 'healthy', are referred to the adjacent non-tumoural zone of the same patients ($n = 19$). Human studies were approved by the Ethical Committee of the University of Naples Federico II, and all patients enrolled for this study provided written informed consent.

### 2.2 | Gene Expression across Normal and Tumour tissue (GENT) data analysis

Relative gene expression values were obtained from the interrogation of the Gene Expression across Normal and Tumour tissue (GENT2) database (Park et al., 2019), in which the NAAA relative transcript levels of CRC and healthy control samples were available.

The query output values were divided into healthy (Accession ID: E-TAMB-118, E-TAMB-176, GSE4107, GSE4183, GSE7307, GSE8671, GSE9254, GSE9452, GSE9686, GSE10191, GSE10616, GSE11831, GSE13367, GSE13471, GSE14580, GSE15960, GSE18426, GSE19963, GSE20916, GSE21510, GSE32323, GSE37267, GSE37364, GSE38713, GSE39397, GSE40220, GSE40967, GSE41328, GSE43346 and GSE62932; $n = 397$) and tumoural samples (Accession ID: GSE2109, GSE4107, GSE4183, GSE4554, GSE8671, GSE13067, GSE13294, GSE13471, GSE14333, GSE14580, GSE15960, GSE17536, GSE17537, GSE18088, GSE18462, GSE19860, GSE20916, GSE21510, GSE23194, GSE26027, GSE26682, GSE26906, GSE27157, GSE29623, GSE30540, GSE31595, GSE32323, GSE33114, GSE34489, GSE35144, GSE35452, GSE35603, GSE35896, GSE37364, GSE37892, GSE38832, GSE39084, GSE40367, GSE40967, GSE41328, GSE43576, GSE52847, GSE54483, GSE60697, GSE62080, GSE62932, GSE64258, GSE64857, GSE71222 and GSE73883; $n = 3775$) in order to analyse the difference of NAAA expression level.

### 2.3 | Measurements of N-Acylethanolamines (NAEs)

Frozen tissues derived from human specimens and from xenografted murine tumours were homogenized in chloroform/methanol/Tris–HCl 50 mM, pH 7.4 (2:1:1, v/v), containing 5 pmol of [$^2$H]$_8$-anandamide, 50 pmol of [$^2$H]$_4$-PEA and [$^2$H]$_2$-OEA (Cayman Chemical, Vinci, Italy). The extract was purified by means of silica gel mini-columns, and the eluted fraction containing anandamide, PEA and OEA was analysed by means of LC–atmospheric pressure chemical ionization–MS (LC–APCI–MS). Lipid amounts, expressed as pmol, were normalized per gram or milligram of wet tissue (Iannotti et al., 2018).

### 2.4 | In vivo tumour models

#### 2.4.1 | Animals

All the mice reported in present study were housed at the conventional animal house of the Department of Pharmacy, University of Naples Federico II (Naples, Italy) and kept in cages supplemented with environmental enrichment. For the xenograft model, 6- to 8-week-old female BALB/c nude mice were used (Charles River, Sant'Angelo Lodigiano, Italy), fed ad libitum with sterile mouse food and maintained in pathogen-free conditions in IVC cages. For the azoxymethane model, 6-week-old male CD1 background mice (Charles River, Sant'Angelo Lodigiano, Italy) were used and fed ad libitum with standard food (Mucedola srl, Settimo Milanese, Italy) and maintained in open cages with free access to water. All the animals were anaesthetized by enflurane inhalation before being humanely killed by carbon dioxide. The death was further ensured by confirmation of rigor mortis. All efforts were made to minimize the number of animals used and

their suffering. Mice were blindly randomized, and experimental procedures and protocols were in compliance with national (Direttiva 2010/63/UE) laws and policies and approved by the Italian Ministry of Health. Animal studies are reported in compliance with the ARRIVE guidelines (Percie du Sert et al., 2020) and with the recommendations made by the British Journal of Pharmacology (Lilley et al., 2020).

### 2.4.2 | Xenograft model

Tumour xenograft model of CRC was established using BALB/c nude mice (Charles River, Sant'Angelo Lodigiano, Italy). The effect of the NAAA inhibitor AM9053 was evaluated on tumour formation induced by the subcutaneous injection of HCT116 cells ($2.5 \times 10^6$, 200-μl PBS) into the back of the mice. AM9053, at the dose of 20 mg·kg$^{-1}$ (Alhouayek et al., 2015), was given peritumourally three times per week, tumour size measured and calculated for all the duration of the experiment (Romano et al., 2019). At 15 days after treatment started, mice were humanly killed, and tumours were excised, photographed, weighed and processed.

### 2.4.3 | Azoxymethane model

Azoxymethane (40 mg·kg$^{-1}$ in total, i.p.) (Sigma-Aldrich, Milan, Italy) was administered in male CD1 background mice (Charles River, Sant'Angelo Lodigiano, Italy) at the single dose of 10 mg·kg$^{-1}$, once *per* week for 4 weeks. AM9053 (20 mg·kg$^{-1}$, i.p.) (Alhouayek et al., 2015) was given intraperitoneally three times per week, starting 1 week before the first administration of azoxymethane. All animals were anaesthetized by enflurane inhalation before being killed by asphyxiation with $CO_2$ after 12 weeks the first injection of azoxymethane, right time for the development of aberrant crypt foci (ACF), polyps and tumours (Izzo et al., 2008). Detection and quantization of aberrant crypt foci, polyps and tumours on the colon were performed as previously reported (Izzo et al., 2008).

### 2.5 | Transcript analysis by quantitative PCR

mRNA obtained from human tissues, xenografted murine tumours and/or human cell lines was extracted by using PureZOL Reagent (Bio-Rad, Segrate, Italy), following the manufacturer's instructions. Reverse transcription was performed by using the High-Capacity cDNA Reverse Transcription Kit (Applied Biosystems, Waltham, MA, USA), and RT-PCR was completed using SYBR Green Master Mix (Applied Biosystems, Waltham, MA, USA) and gene specific primers, as detailed in Table S1. All the data were normalized to the housekeeping gene S16 and/or GAPDH, and the relative abundance was expressed by using the $2^{-\Delta Ct}$ formula.

### 2.6 | Immunofluorescence

Frozen sections (10 μm) in Cryobloc Compound (Diapath, Martinengo, Italy) of tumour explanted from xenograft tumour-bearing mice, treated or not with the NAAA inhibitor AM9053 (20 mg·kg$^{-1}$, peritumourally), were fixed in 4% paraformaldehyde and then blocked with PBS containing 2% BSA, 2% goat serum and 0.1% Triton (all from Sigma-Aldrich, Milan, Italy) for 60 min at room temperature and incubated overnight at 4°C with the human anti-Ki67 (1:400, Abcam, Cambridge, UK). All sections were then incubated for 30 min at room temperature with Alexa Fluor 594-conjugated goat anti-rabbit IgG (1:1000; Jackson ImmunoResearch, Cambridge, UK), followed by incubation for 5 min at room temperature with DAPI (1:25,000; Invitrogen, Waltham, MA, USA). Sections were mounted with glycerol (Sigma-Aldrich, Milan Italy) and acquired/analysed by using Axio Imager M2P combined with high-end fluorescence imaging system ApoTome.2 (Zeiss, Jena, Germany). Images were acquired with an objective 20×.

### 2.7 | Western blot

The Immuno-related procedures used comply with the recommendations made by the *British Journal of Pharmacology* (Alexander et al., 2018). Xenograft samples derived from tumour-bearing mice, treated or not with AM9053, were pounded in liquid nitrogen and lysed in RIPA buffer (10-mM Tris–Cl [pH 8.0],1-mM EDTA, 140-mM NaCl, 1% Triton X-100, 0.1% [v/v] sodium deoxycholate and 0.1% SDS) supplemented with protease (Roche, Monza, Italy) and phosphatase inhibitors (Sigma-Aldrich, Milan, Italy); 50 μg of protein extracts was fractionated by 8% SDS-PAGE according to the manufacturer's protocols (Bio-Rad, Segrate, Italy). After incubation with 5% (w/v) non-fat milk in TBS-T (10-mM Tris, pH 8.0, 150-mM NaCl and 0.5% [v/v] Tween 20) for 60 min, the membranes were incubated overnight with fresh PathScan® Multiplex Western Cocktail (Rabbit, 1:1000, Cell Signalling, Catalogue Number 5301, Danvers, MA, USA), and thereafter, fresh secondary antibody anti-rabbit IgG (1:2500, Promega, Catalogue Number S3731, Milan, Italy), linked to HRP, was added. The signal was visualized by enhanced chemiluminescence using Chemidoc XRS (Bio-Rad, Segrate, Italy) and analysed using Quantity One Software Version 4.6.8. Ras-related protein (Rab-11) was used as housekeeping normalizing protein.

### 2.8 | Tumour secretome collection

Tumour-bearing nude mice treated or not with the NAAA inhibitor AM9053 (20 mg·kg$^{-1}$) were killed with enflurane/$CO_2$ 15 days after treatment starting, tumours excised and cultured in DMEM, without FBS, for 24 h. The conditioned mediums were collected and added to HCT116 or Caco-2 cells for 24 h at 37°C. Thereafter, CRC cells were washed in PBS and used for further analyses.

## 2.9 | Oncogenic array

Tumour secretomes collected (as above stated) from tumour-bearing nude mice, treated or not with AM9053, were analysed by using the oncogenic array Proteome Profiler Human XL Oncology Array Kit (R&D Systems, Minneapolis, MN, USA) following the manufacturer's instructions.

## 2.10 | Cell lines

The human colon adenocarcinoma cell lines (i.e., HCT116 and Caco-2) (ATCC from LGC Standards, Milan, Italy) and the immortalized healthy human colonic epithelial cells (HCEC), derived from human colon biopsies, kindly gifted from Fondazione Callerio Onlus (Trieste, Italy), were cultured in DMEM (Sigma-Aldrich, Milan, Italy) supplemented with 10% and heat-inactivated FBS (Sigma-Aldrich, Milan, Italy). Cell lines were maintained at 37°C in a humidified incubator with 5% $CO_2$, and their viability was evaluated by trypan blue exclusion. All the cell lines used were free from mycoplasma contamination.

## 2.11 | Cell viability assay

Cell viability was evaluated by measuring the neutral red uptake (NR assay) as previously described (Romano et al., 2014). Briefly, cells (HCT116 and HCEC) ($1.5 \times 10^4$ cells seeded in a 96-well plate) treated or not with AM9053 (0.1–3 μM, 24 h) were incubated with NR dye solution (50 μg·ml$^{-1}$ in 10% FBS) for 3 h at 37°C and then lysed with 1% acetic acid. The absorbance was read at 532 nm (iMarkTM microplate reader, Bio-Rad, Segrate, Italy). All results are expressed as percentage of cell viability.

## 2.12 | Bromodeoxyuridine incorporation assay

Cells (HCT116, Caco-2, HCEC and siNAAA-HCT116) ($1.0 \times 10^4$ cells seeded in a 96-well plate), allowed to adhere (24 h) and starved overnight by serum deprivation, were then treated for 24 h with AM9053 (0.1–3 μM [HCT116] and 3 μM [Caco-2, HCEC and siNAAA-HCT116]) and incubated with bromodeoxyuridine (BrdU; 10 μM) in the cell medium for 2 h. Cell proliferation was then detected using the bromodeoxyuridine proliferation ELISA kit (Roche, Monza, Italy) following the manufacturer's protocol.

Using this assay, the antiproliferative effect of AM9053 was evaluated (in HCT116 cells) in the presence of GW6471 (3 μM, PPAR-α antagonist) (Alexander, Cidlowski, et al., 2021), 5′-iodoresiniferatoxin (0.1 μM, transient receptor potential vanilloid 1 [TRPV1] antagonist) (Alexander, Mathie, et al., 2021), and AM251 and AM630 (both 1 μM, CB$_1$ and CB$_2$ receptor antagonists, respectively) (Alexander, Christopoulos, et al., 2021) (all from Tocris, distributed by Bio-Techne, Milan, Italy) and incubated 30 min before AM9053 (3 μM). The results are expressed as percentage of cell proliferation.

## 2.13 | Cell cycle analysis

Cell cycle analysis was performed according to BD Pharmingen™ bromodeoxyuridine Flow Kit (BD Biosciences, Milan, Italy) and conducted on HCT116 cells and/or siNAAA-HCT116 ($1.5 \times 10^5$ cells seeded in a six-well plate), overnight serum deprived and treated or not with AM9053 (3 μM) for 24 h. Cells were revealed by using Bri-Cyte flow cytometer (Mindray, Trezzano sul Naviglio, Italy), gated based on forward and side scatter to separate debris, and then the cellular events were further gated based on their bromodeoxyuridine and 7-aminoactinomycin D content. Data were analysed by FlowJo v10 software (Tree Star, Ashland, OR, USA) and expressed as fold change of the cells in each cell cycle phase.

## 2.14 | Scratch assay

The scratch assay was performed on subconfluent HCT116 and/or Caco-2 trypsinized and plated on μ-Dish 35-mm culture inserts (ibidi GmbH, Gräfelfing, Germany) ($5 \times 10^4$ per 70 μl per area). After 24 h, inserts were gently removed by sterile tweezers and a scratch was made in the monolayers. Cells were then incubated with mitomycin C 30 μg·ml$^{-1}$ (Sigma-Aldrich, Milan, Italy) in serum-free media, in order to completely inhibit cell proliferation. After 2 h, CRC cells were treated with AM9053 (3 μM, 24 h). Using this assay, the effect of AM9053 on HCT116 cell migration was also evaluated in the presence of GW6471 (3 μM, PPAR-α antagonist), 5′-iodoresiniferatoxin (0.1 μM, TRPV1 antagonist), and AM251 and AM630 (both 1 μM, CB$_1$ and CB$_2$ antagonists, respectively) (all from Tocris, distributed by Bio-Techne, Milan, Italy) and incubated 30 min before AM9053 (3 μM).

Wound area recovery was observed under a phase-contrast microscope (Leica, Wetzlar, Germany) and photographed at Time 0 point (right after the mitomycin C removal) and after 24 h from the pharmacological treatment. The size of the opened area was measured by Fiji (NIH) software. Two images were acquired for each well, and at least three replicates were analysed for each treatment. The results are expressed as % of scratch closure (Time 0 area − 24-h area/Time 0 area * 100).

## 2.15 | Transfection

HCT116 cells ($1.5 \times 10^5$ cells seeded in a six-well plate) were transfected with siRNA for NAAA (Trilencer-27 siRNA duplex, OriGene, Rockville, MD, USA) (10 nM) and/or a standard negative control (5 nM), resuspended in MegaTran 2.0 Transfection Reagent (OriGene, Rockville, MD, USA) and Opti-MEM® (Thermo Fisher Scientific, Waltham, MA, USA) in a total volume of 100 μl and added drop by drop to cells for 4 h. The transfection was then stopped by adding DMEM supplemented with 20% FBS overnight and replaced with complete culture medium incubated at 37°C, 5% $CO_2$ for 48 h. Silencing efficiency was controlled by performing RT-PCR, and the obtained siNAAA-HCT116 was used as due.

## 2.16 | Materials

AM9053 (10-isothiocyanatodecyl benzene) was synthesized as previously described-(Malamas et al., 2015). All the reagents for in vitro cell cultures and western blot analysis were provided by Sigma-Aldrich (Milan, Italy), Aurogene (Rome, Italy) and/or Bio-Rad (Segrate, Italy). The vehicles used for in vivo (10% ethanol, 10% Tween 20 and 80% saline, 2 ml·kg$^{-1}$) and in vitro (0.1% ethanol) experiments had no effect on the responses under the study.

## 2.17 | Data and analysis

The data and statistical analysis comply with the recommendations of the *British Journal of Pharmacology* on experimental design and analysis in pharmacology (Curtis et al., 2018). The study was designed to generate groups of equal size, using randomization and blinded analysis. All data are expressed as mean ± SD, and GraphPad Prism 7 software was used to perform statistical analysis. Outliers were identified by ROUT test. The D'Agostino and Pearson (≥8$n$ per group) or Shapiro–Wilk (≤8$n$ per group) tests were used to determine if a data set was well modelled by a normal distribution or not. To determine differences between two normal groups' comparison, data were tested using unpaired and/or paired Student's $t$-test, and no-normal groups were statistically compared with Mann–Whitney test. For multiple-group comparisons, normal data were compared via one-way ANOVA with Dunnett's post hoc test and/or with Tukey's post hoc test analysis, and non-normal data were compared via Kruskal–Wallis with Dunn's test. To determine differences between groups with multiple factors, data were tested using two-way ANOVA followed by Bonferroni's test. Post hoc tests were run only when $F$ achieved $P < 0.05$ and there was no variance inhomogeneity. All measurements were undertaken only for $n \geq 5$.

## 2.18 | Nomenclature of targets and ligands

Key protein targets and ligands in this article are hyperlinked to corresponding entries in the IUPHAR/BPS Guide to PHARMACOLOGY http://www.guidetopharmacology.org and are permanently archived in the Concise Guide to PHARMACOLOGY 2021/22 (Alexander, Christopoulos, et al., 2021; Alexander, Cidlowski, et al., 2021; Alexander, Kelly, et al., 2021; Alexander, Mathie, et al., 2021).

## 3 | RESULTS

### 3.1 | NAAA pharmacological inhibition impacts CRC growth and development in vivo

In order to investigate the functional role of NAAA in in vivo CRC growth, we first used the xenograft model of CRC, in which a subcutaneous (s.c.) injection of HCT116 cells (constitutively expressing NAAA

[threshold cycle—Ct ± SD: NAAA 25.3 ± 0.287; GAPDH 17.24 ± 0.191, $n = 6$]) in the back of immunodeficient BALB/c mice establishes a well-known method to evaluate tumour growth (Romano et al., 2019). AM9053, a selective, potent and slowly reversible NAAA inhibitor (IC$_{50}$ = 30 nM), suggested as a useful tool compound to study NAAA functions (Bottemanne et al., 2018) and previously used for systemic administrations (Alhouayek et al., 2015), was injected peritumourally every 2 days (20 mg·kg$^{-1}$). As shown in Figure 1a, 15 days after its first administration (corresponding to seven measurements), AM9053 determined a significative reduction of the xenograft tumour volume compared with the vehicle group. Consistently, *post-mortem* excited and photographed tumours of AM9053-treated mice were smaller (representative images reported in Figure 1b), and weights were significantly lower than the vehicle-treated ones (Figure 1c).

NAAA inhibition by AM9053 has been previously shown to increase NAE levels (Bottemanne et al., 2018), with changes of specific NAEs depending on the disease as well as on the tissue analysed. In our scenery, CRC xenograft tumours showed a significant increase of OEA levels (Figure 1d), whereas PEA and anandamide levels were not altered (Figure 1e,f). Quantitative RT-PCR (qRT-PCR) analysis performed on explanted tumours revealed that AM9053 did not alter significantly PPAR-α, TRPV1 and CB receptor gene expression (Figure S1A–D). In order to understand the pathways associated to tumour growth decrease, observed after NAAA pharmacological inhibition, we next examined the expression of Ki-67 as well as pAKT, ERK1/2 and pS6 in the xenograft frozen tumour sections and protein lysates, respectively. High-end immunofluorescence images reported in Figure 1g revealed that frozen sections of AM9053-treated tumours contained a significantly fewer number of red Ki-67-positive cells (lower images) than vehicle-treated tumours (upper images) as also corroborated by the intensity mean value of the red positive cells (Figure 1h). On the other hand, exploratory data showed that AM9053 treatment did not alter the expression of the proteins (i.e., pAKT, ERK1/2 and pS6) involved in the main proliferative pathways (representative western blot images reported in Figure S1E).

The role of NAAA inhibition in reducing tumour development was further supported by using the azoxymethane model of colon cancer, a well-known method to induce an experimental sporadic colon cancer (Neufert et al., 2007). Here, we observed that AM9053 (20 mg·kg$^{-1}$), injected intraperitoneally every 2 days for 13 weeks, reduced, approximately by 40%, the number of azoxymethane-induced tumours (Figure S1F).

In summary, we conclude that NAAA is functionally relevant in CRC development and its pharmacological inhibition counteracts tumour growth by reducing the proliferative marker Ki-67 *in vivo*.

### 3.2 | The NAAA inhibitor-treated tumour secretome shows altered expression of members belonging to the EGF family

The tumour secretome is constituted by several factors that, released from tumoural cells as well as from other types of cells interacting
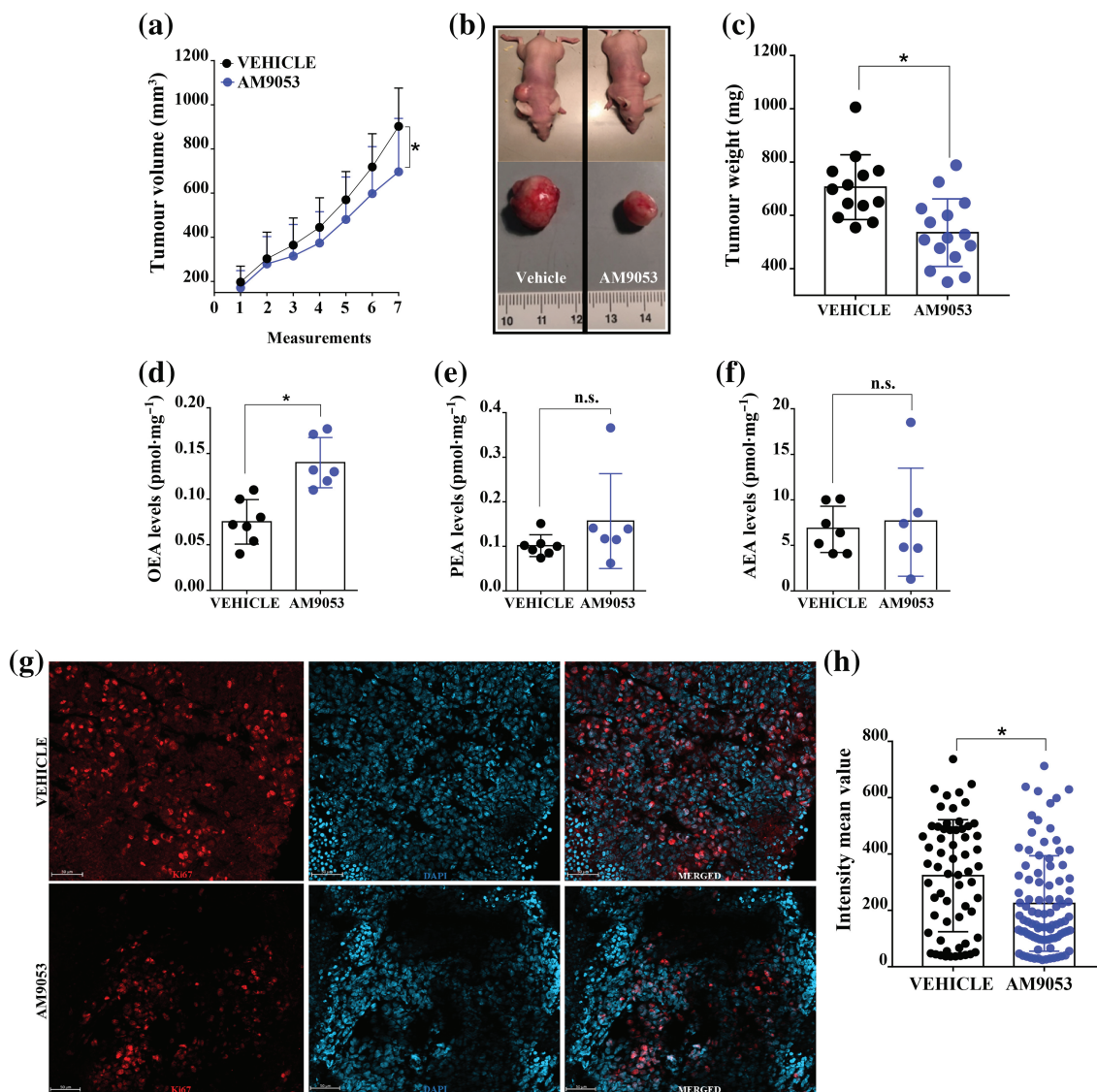
**FIGURE 1** N-acylethanolamine acid amidase (NAAA) selective inhibition reduces CRC growth *in vivo*. (a) Effect of the NAAA inhibitor AM9053 (20 mg·kg$^{-1}$, peritumourally) on in vivo tumour growth, measured as tumour volume (mm$^3$), over a 15-day period (seven measurements). Each dot represents the mean ± SD of 13 mice for vehicle and 15 mice for AM9053 experimental groups; *$P < 0.05$ versus vehicle by two-way ANOVA. (b) Representative macroscopic pictures of tumour-bearing mice (upper images) as well as of the explanted tumours (lower images), with the respective treatments, at the day of the kill. (c) Weights (reported in mg) of the xenograft tumours explanted from tumour-bearing mice treated ($n = 15$) or not ($n = 13$) with AM9053 (20 mg·kg$^{-1}$, peritumourally). (d–f) Endogenous-level measurements of NAEs: N-oleoylethanolamine, OEA (d), N-palmitoylethanolamine, PEA (e) and anandamide (AEA) (f) in mouse xenograft tumours treated ($n = 6$) or not ($n = 7$) with AM9053 (20 mg·kg$^{-1}$, peritumourally). The levels of NAEs are reported as pmol·mg$^{-1}$ of wet tissue weight. (g) Representative high-end fluorescence images of Ki-67 expression in frozen sections of tumours explanted from tumour-bearing mice treated (lower images) or not (upper images) with AM9053 (20 mg·kg$^{-1}$, peritumourally). Ki-67 staining is visualized in red, and nuclei were counterstained with DAPI in blue. Magnification: 20× (white scale bar 50 μm). (h) Graph showing the intensity mean value (±SD) of red Ki-67-positive cells. Values are expressed as means ± SD; *$P < 0.05$ versus vehicle, as assessed by Student's *t* test; n.s., not significant

with them, contribute in promoting and sustaining tumour growth (Xue et al., 2008). Therefore, in order to enforce the functional role of NAAA in tumour growth, we collected the secretome from tumour xenografts as illustrated by the schematic representation reported in Figure S2A. Of note, a preliminary data revealed that tumour secretome determined a down-regulation trend of NAAA expression in HCT116 cells (Figure S2B) as well as in another adenocarcinoma cell line, the Caco-2 cells (Figure S2C), which expresses NAAA (basal NAAA expression: Ct ± SD: NAAA 26.37 ± 0.295; GAPDH 17.95 ± 0.259, $n = 6$). To further examine the molecular mechanisms driving the reduction of tumour growth induced by the pharmacological NAAA inhibition, we analysed the tumour secretome obtained from xenograft mice treated or not with AM9053 by performing an analysis of the global changes in protein expression. By using a well-controlled

and commercially available oncogenic proteome array, we found consistent alterations in the protein expression levels of Erb-B1, Erb-B2, Erb-B3 and AREG in tumour secretomes derived from mice treated with AM9053 (Figure S2D). Of interest, all these proteins are members of the EGF family, and their role as master regulators of tumour cell proliferation is well established (Yarden & Sliwkowski, 2001). Collectively, NAAA inhibition impacts the composition of the tumour secretome, which, in turn, negatively affects the expression of members belonging to the EGF family.

## 3.3 | AM9053 inhibits tumoural cell proliferation via TRPV1 and PPAR-α

The data described above prompted us to deepen our understanding of AM9053 action on CRC cells *in vitro*. First, AM9053, at concentrations ranging from 0.1 to 3 μM, did not exert cytotoxic effects neither in tumoural HCT116 (Figure 2a 1) nor in healthy HCEC (Figure 2b 1). Subsequently, by using the bromodeoxyuridine incorporation assay, we tested the antiproliferative effect of the NAAA inhibitor on HCT116 cells (i.e., the same colorectal adenocarcinoma cell line used

to induce xenograft tumours). Of interest, our results revealed that AM9053 (0.1–3 μM) reduced the proliferation rate after 24 h of exposure (Figure 2c) with an $IC_{50}$ value ± SD of 1.056 ± 0.285 μM. The antiproliferative effects of AM9053 (3 μM, 24 h exposure) were also confirmed in Caco-2 cells (% Caco-2 cell proliferation, mean ± SD: control 100 ± 4.14; AM9053 3 μM 80.95 ± 12.02; $n = 7$, $P < 0.01$). By contrast, AM9053 (3 μM, 24-h exposure) did not affect the proliferation rate of the healthy HCEC line (Figure 2d), which also expresses NAAA (NAAA expression [Ct ± SD: NAAA 26.13 ± 0.155; GAPDH 17.46 ± 0.17, $n = 6$]). These results emphasize the role of NAAA in tumoural—but not in healthy—cell proliferation.

In order to determine the pharmacological mechanism of action underlying the observed antiproliferative effect of NAAA inhibition, we treated HCT116 with AM9053 in the presence of selective antagonists of the main targets responsible for NAE action (Di Marzo & Piscitelli, 2015) (i.e., GW6471 [PPAR-α antagonist] [Alexander, Cidlowski, et al., 2021], 5′-iodoresiniferatoxin [TRPV1 antagonist] [Alexander, Mathie, et al., 2021], AM251 [CB1 antagonist] and AM630 [CB2 antagonist] [Alexander, Christopoulos, et al., 2021]). Interestingly, we found that the antiproliferative effect of AM9053 was significantly reverted by PPAR-α and TRPV1, but not by CB1 and
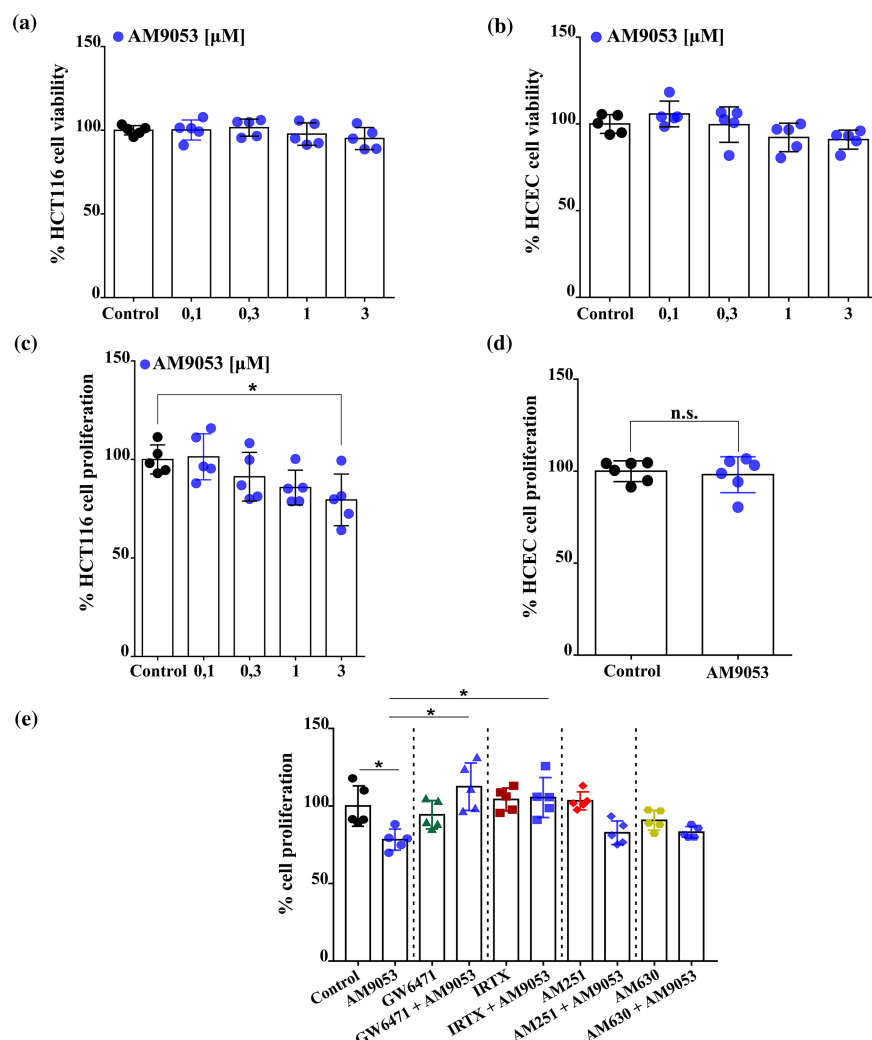


**FIGURE 2** The *N*-acylethanolamine acid amidase (NAAA) selective inhibitor AM9053 affects tumour cell proliferation. (a) Cell viability assay in HCT116 and (b) in healthy human colonic epithelial cells (HCEC) alone or in the presence of AM9053 (0.1–3 μM, 24 h) ($n = 5$). Results are expressed as mean ± SD. (c) Cell proliferation rate of HCT116 cells incorporating bromodeoxyuridine (BrdU), alone or in the presence of AM9053 (0.1–3 μM, 24 h). Results are expressed as percentage of cell proliferation ($n = 5$ independent experiments). Values are expressed as means ± SD; *$P < 0.05$ versus control, as assessed by one-way ANOVA followed by Dunnett's multiple comparisons test. (d) Cell proliferation rate of HCEC incorporating BrdU, alone or in the presence of AM9053 (3 μM, 24 h). Results are expressed as percentage of cell proliferation ($n = 6$). Values are expressed as means ± SD; n.s., not significant as assessed by unpaired Student's *t*-test. (e) The antiproliferative effect of AM9053 (3 μM) was also evaluated in the presence of GW6471 (3 μM, PPAR-α antagonist), 5′-iodoresiniferatoxin (I-RTX 0.1 μM, TRPV1 antagonist), AM251 (1 μM, CB1 antagonist) and AM630 (1 μM, CB2 antagonist). All results are expressed as percentage of cell proliferation ($n = 5$ independent experiments) and as means ± SD; *$P < 0.05$ versus control and/or AM9053 as assessed by one-way ANOVA followed by Tukey's multiple comparisons test

CB2 antagonists (Figure 2e). Overall, these results suggest that the antiproliferative effects of NAAA pharmacological inhibition are at least in part mediated by PPAR-α and TRPV1.

## 3.4 | AM9053 promotes cell cycle arrest in the S phase and reduces cell migration

Next, we explored the influence of AM9053 on HCT116 cell cycle progression by using bromodeoxyuridine/7-ADD staining. As shown in Figure 3a and in the representative density plots reported in Figure 3b, a significantly higher percentage of cells in the S phase was observed in AM9053-treated cells than in the control group, with a concomitant

significant reduction in the proportion of cells in the G0/G1 phase. These data suggest that the inhibition of tumoural cell growth is associated with the induction of the S-phase cell cycle arrest.

Cyclin A2 is essential during the S phase when it activates **cyclin-dependent kinase 2 (CDK2)** as well as in regulating the initiation and progression of DNA synthesis (Heichman & Roberts, 1994). In agreement with the blockade of the S phase, AM9053 reduced both cyclin A2 (Figure 3c) and CDK2 (Figure 3d) expression, whereas it did not affect cyclin B1 (Figure 3e) and **cyclin-dependent kinase 1 (CDK1)** (Figure 3f), which are known to regulate the G2/M phase.

Moreover, AM9053 significantly decreased the migration of HCT116 (Figure S3A) and Caco-2 (Figure S3B) cells, when their
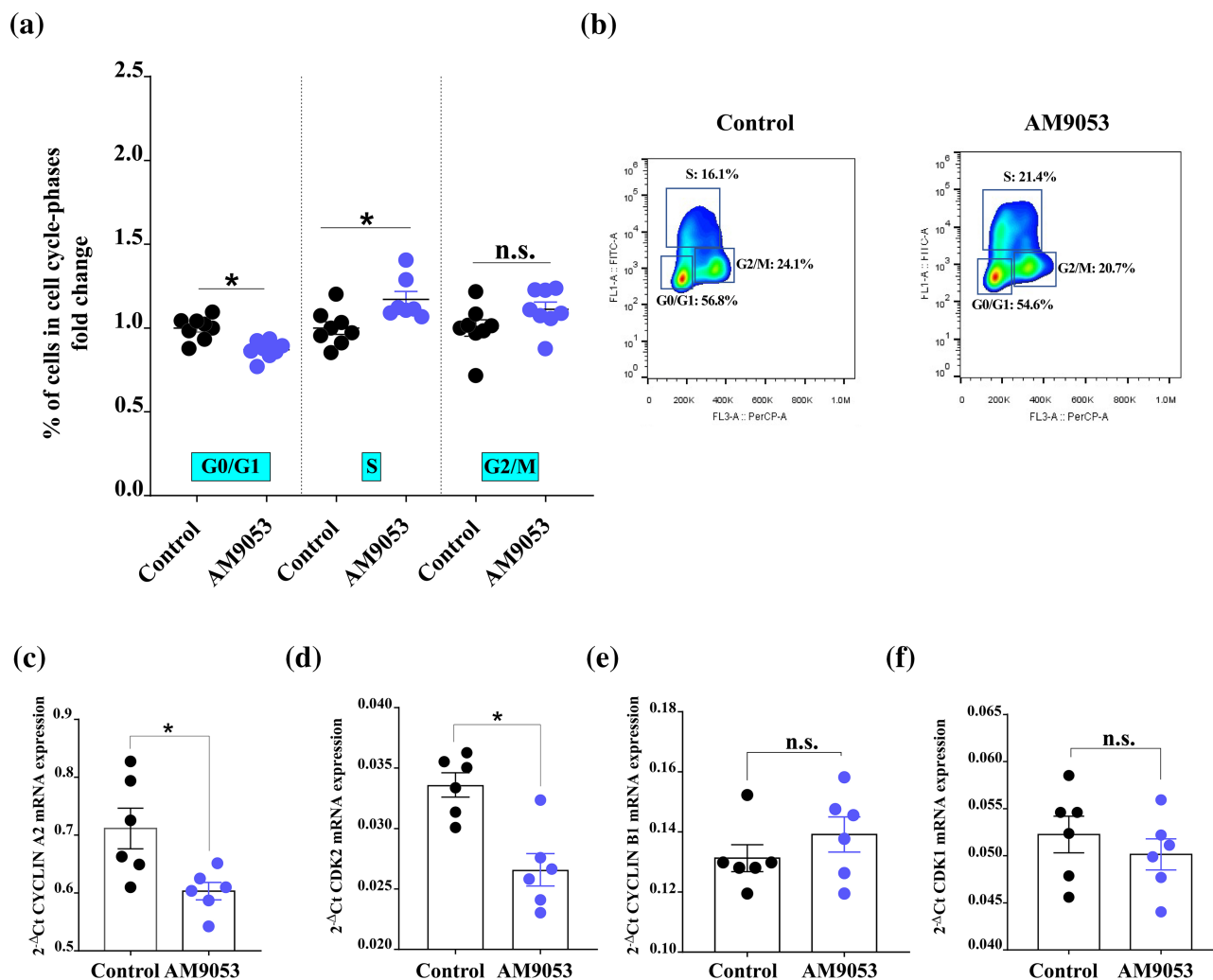


**FIGURE 3** The inhibitor AM9053 blocks tumoural cell cycle. (a) Cell cycle analysis by flow cytometry of HCT116 cells treated or not with AM9053 (3 μM, 24 h). Results are expressed as fold change of the cells in each cell cycle phase ($n = 8$ independent experiments) in order to uniform the % values of the cells in each phase of the cell cycle ($n = 1$ outlier has been removed by ROUT test). Values are expressed as means ± SD; *$P < 0.05$ versus control, as assessed by unpaired Student's $t$ test and/or Mann–Whitney test. (b) Representative density plots and cell percentage, indicating the G0/G1-, G2/M- and S-phase distribution of HCT116 cells treated (right figure) or not (left figure) with AM9053 (3 μM, 24 h). Gene expression, in HCT116 cells, alone or in the presence of AM9053 (3 μM, 24 h), of cyclin A2 (c), cyclin-dependent kinase 2 (CDK2) (d), cyclin B1 (e) and cyclin-dependent kinase 1 (CDK1) (f). Gene expression was measured by qRT-PCR and calculated by using the $2^{-\Delta Ct}$ formula ($n = 6$ independent experiments). Values are expressed as means ± SD; *$P < 0.05$ versus control and analysed by Student's $t$-test; n.s., not significant

proliferation was blocked by pretreatment with mitomycin C. Contrary to the data on cell proliferation (Figure 2d), the effect of AM9053 on migration was not affected by the PPAR-α or TRPV1 antagonists (Figure S3C). These results suggest that NAAA inhibition may play a role not only in proliferation but also in migration, although with a different mode of action (i.e. TRPV1 and PPAR-α involvement in proliferation but not in migration).

Altogether, these results point out the prominent role of NAAA in CRC cell growth. The antiproliferative effect of NAAA inhibition is mediated by PPAR-α and TRPV1 and is dependent on cell cycle arrest in the S phase, probably due to cyclin A2/CDK2 down-regulation.

## 3.5 | Transient NAAA knock-down results in antiproliferative effects

To determine whether the silencing of NAAA was able to mimic the antiproliferative effects caused by NAAA pharmacological inhibition, HCT116 cells were efficiently knocked down for NAAA (siNAAA-HCT116) by using siRNA (Figure 4a). NAAA silencing did not affect HCT116 cell viability over 72 h in comparison with treatment with siRNA scrambled sequence (data not shown), but, importantly, it significantly reduced cell proliferation compared with the scramble control (Figure 4b). Additionally, AM9053 did not produce significant antiproliferative effects in siNAAA-HCT116 cells, thus confirming NAAA involvement and the selectivity of NAAA inhibitor AM9053 (Figure 4b). In agreement with the effects exhibited by AM9053, siNAAA-HCT116 cells exhibited a significantly higher percentage of cells in the S phase, with a parallel reduction in the proportion of cells in the G0/G1 phase (Figure 4c and representative dot plots in Figure 4d). Accordingly, this effect was associated to the reduction in cyclin A2 expression (Figure 4e), despite no change in CDK2 expression (Figure 4f). Similarly, no effect on the expression of cyclin B1 (Figure 4g) and CDK1 (Figure 4h) regulating the G2/M phase was observed. Taken together, these results strongly support and indicate a prominent role of NAAA in influencing CRC cell cycle and proliferation.

## 3.6 | NAAA expression is reduced in human CRC tissues and this reduction is associated with an augmentation of its substrates

The last aim of this study was to compare NAAA expression in primary human colon cancer tissues versus the adjacent non-tumour counterparts. Our results show that the mRNA levels of NAAA quantified in surgically resected colorectal adenocarcinomas were significantly down-regulated (Figure 5a). According to the tumour–node–metastasis staging system (Edge & Compton, 2010), tumours were classified as pT2, pT3 and pT4, and interestingly, we observed that NAAA expression decreased significantly only in stages pT2 and pT3 with no changes observed in pT4 tumours (Figure 5b). These findings were corroborated by the analysis of human CRC samples available in

the public gene expression GENT2 database (Park et al., 2019), in which we found a significant decline of NAAA relative transcript levels in all CRC samples available (Figure 5c). Because NAAA hydrolyses PEA, OEA and anandamide (Bottemanne et al., 2018), our next step was to quantify its substrates in human CRC specimens ($n = 8$) versus their healthy counterparts ($n = 8$). We found that the significant NAAA reduction observed in CRC tissues was associated with a significant increase of PEA, OEA and anandamide levels (Figure 5d–f). Taken together, these data support the hypothesis that NAAA plays a role in human CRC, its expression being strongly down-regulated with consequent augmentation of the tissue concentrations of its three main substrates.

## 3.7 | NAE main targets are dysregulated in human CRC

Finally, because we found a significative up-regulation of PEA, OEA and anandamide levels in human CRC specimens, we analysed the expression of their main targets, namely, PPAR-α, TRPV1 and cannabinoid ($CB_1$ and $CB_2$) receptors (Di Marzo & Piscitelli, 2015). We found a significant reduction only in the expression of CB receptors (Figure S4A,B), whereas we did not observe any statistical difference in PPAR-α and TRPV1 mRNA expression (Figure S4C,D). Overall, these results indicate that some of the most known targets of NAE are down-regulated in CRC.

## 4 | DISCUSSION

In this research, by studying the function and mechanism of action of NAAA during in vivo colon cancer growth and in vitro cell proliferation as well as by investigating the expression of NAAA in human colorectal biopsies, we provide the first evidence that this enzyme has a crucial role in colon carcinogenesis. To investigate the possible role of NAAA in colon carcinogenesis, we used AM9053, a well-established NAAH inhibitor. AM9053 is active following systemic administration in vivo, and it exerts, via NAAA inhibition, intestinal anti-inflammatory effects in mice (Alhouayek et al., 2015). Tumoural xenograft experiments conducted in our study revealed that AM9053 is able to reduce tumour growth in terms of volume and weight and, concomitantly, a significant increase of OEA, but not of PEA and anandamide, levels. This result is not surprising because NAAA inhibition determines an increase of NAE level that is tissue and pathology specific (Bottemanne et al., 2018). For example, AM9053 more markedly increased OEA levels in macrophages (Alhouayek et al., 2017) and PEA levels in experimental colitis (Alhouayek et al., 2015).

Ki-67 staining has been widely used as a tumour proliferation index, because high levels of this protein are predictive of an increased tumour cell proliferation (Gerdes et al., 1984). Therefore, drugs able to reduce or abolish Ki-67 expression may be considered valuable chemotherapeutic agents. Here, we evidenced that the reduced CRC growth observed in those tumours treated with the
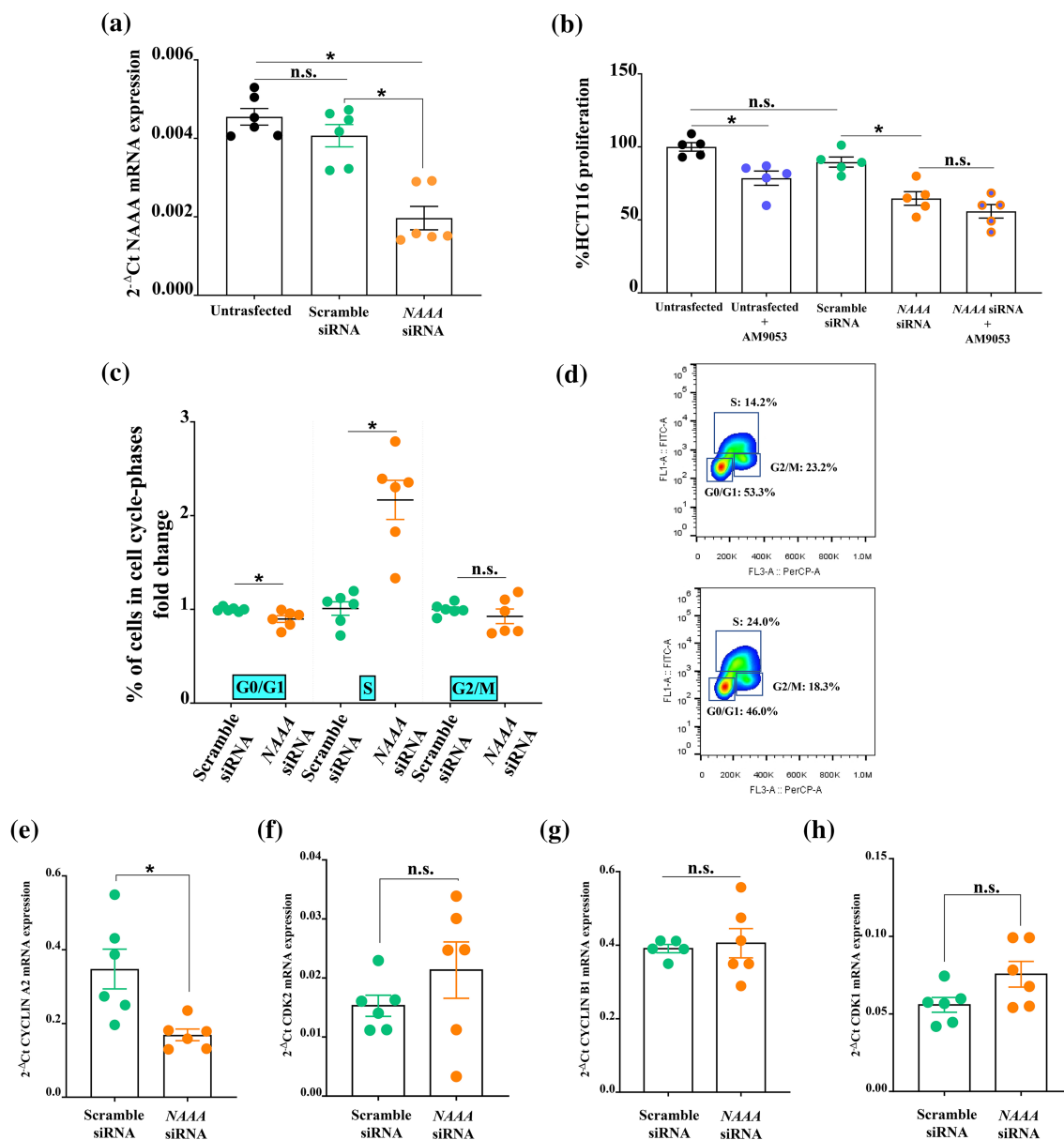
**FIGURE 4** Transient knock-down of *N*-acylethanolamine acid amidase (NAAA) is associated with an antiproliferative effect. (a) *NAAA* gene expression in HCT116 cells alone (untransfected) or in the presence of scramble small interfering (si)RNA and/or NAAA siRNA ($n = 6$ independent experiments). *NAAA* gene expression was measured by qRT-PCR and calculated by using the $2^{-\Delta Ct}$ formula. Values are expressed as means ± SD; *$P < 0.05$ versus scramble siRNA and/or NAAA siRNA as assessed by one-way ANOVA followed by Kruskal–Wallis comparisons test; n.s., not significant. (b) Cell proliferation rate of HCT116 cells incorporating BrdU in the following conditions: alone (untransfected), untransfected in the presence of AM9053 (3 μM, 24 h), scramble siRNA, NAAA siRNA and NAAA siRNA in the presence of AM9053 (3 μM, 24 h). Results are expressed as percentage of cell proliferation ($n = 5$ independent experiments) and as means ± SD; *$P < 0.05$ versus untransfected and/or NAAA siRNA, as assessed by one-way ANOVA followed by Tukey's multiple comparisons test; n.s., not significant. (c) Cell cycle analysis by flow cytometry of HCT116 cells in the presence of scramble siRNA and/or NAAA siRNA. Results are expressed as fold change of the cells in each cell cycle phase ($n = 6$) in order to uniform the % values of the cells in each phase of the cell cycle. Values are expressed as means ± SD; *$P < 0.05$ versus scramble siRNA, as assessed by unpaired Student's *t*-test. (d) Representative density plots and cell percentage, indicating the G0/G1-, G2/M- and S-phase distribution of HCT116 cells in the presence of scramble siRNA (upper figure) and/or NAAA siRNA (lower figure). Gene expression, in HCT116 cells in the presence of scramble siRNA and/or NAAA siRNA, of cyclin A2 (e), CDK2 (f), cyclin B1 (g) and CDK1 (h). Gene expression was measured by qRT-PCR and calculated by using the $2^{-\Delta Ct}$ formula ($n = 6$) ($n = 1$ outlier has been removed by ROUT test for cyclin B1 analysis). Values are expressed as means ± SD; *$P < 0.05$ versus scramble siRNA, as assessed by Student's *t*-test; n.s., not significant

NAAA inhibitor AM9053 was associated with a strong reduction in the number of tumoural Ki-67 proliferative cells, whereas the expression of proteins (i.e., pAKT, ERK1/2 and pS6) involved in the main tumoural proliferative pathways was not altered. Of interest, we also showed that AM9053 reduced the number of tumours in a well-known model of CRC induced by azoxymethane (Neufert et al., 2007),
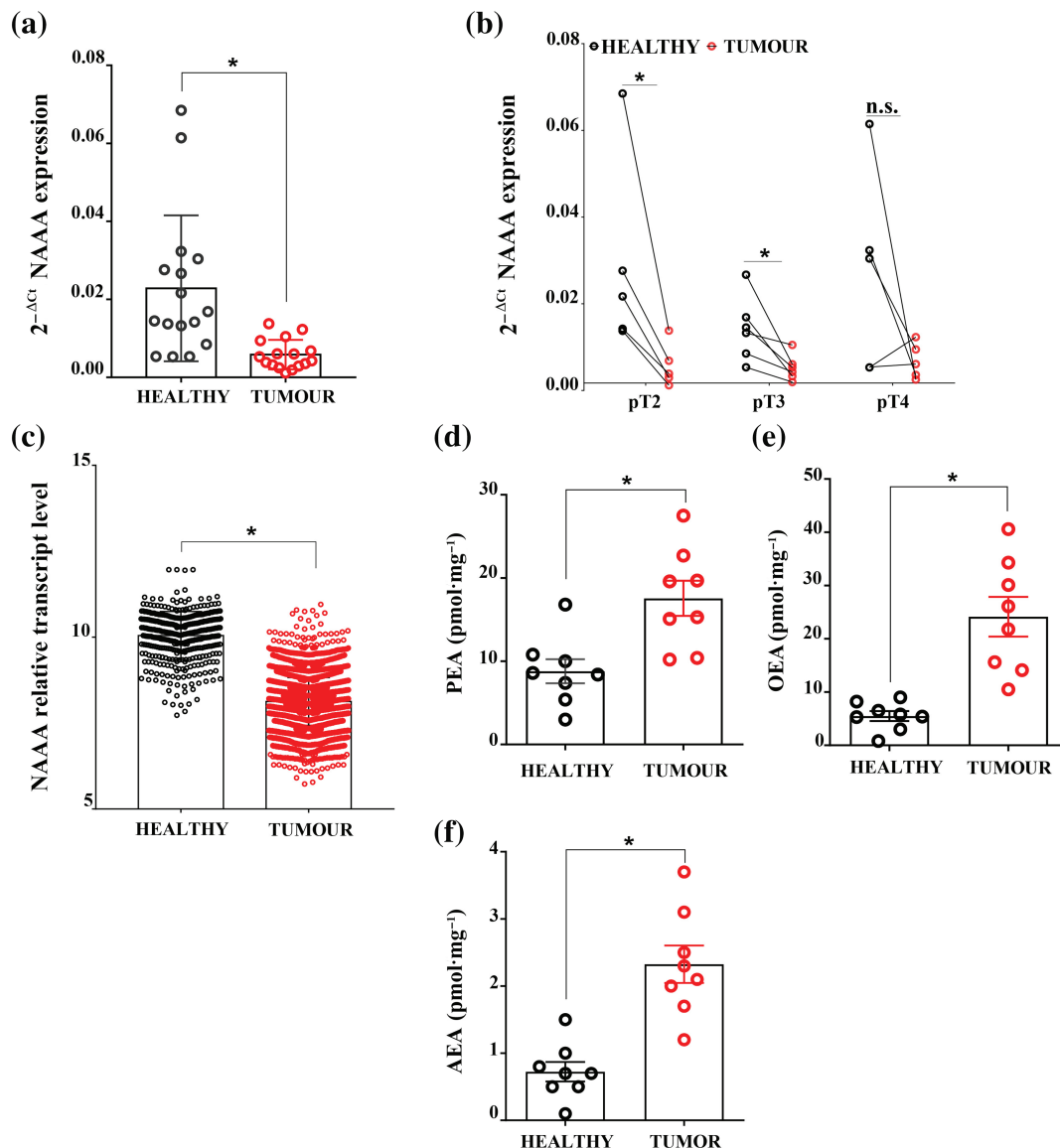
**FIGURE 5** *N*-acylethanolamine acid amidase (NAAA) expression and *N*-acylethanolamine (NAE) levels in human colorectal cancer tissues. *NAAA* gene expression in (a) human colon cancer tissues versus adjacent non-tumour colon specimens (defined as 'healthy') ($n = 16$) and (b) different tumour stages (pT2 [$n = 5$], pT3 [$n = 6$] and pT4 [$n = 5$]) ($n = 3$ outliers have been removed by ROUT test). *NAAA* expression was measured by qRT-PCR and calculated by using the $2^{-\Delta Ct}$ formula. (c) *NAAA* relative transcript levels to housekeeping genes (expressed as log2) in healthy ($n = 393$) and colorectal cancer patients ($n = 3769$) extrapolated from Gene Expression across Normal and Tumour tissue (GENT2) database interrogation ($n = 9$ outliers have been removed by ROUT test). Endogenous-level measurements of *N*-acylethanolamines (NAEs): *N*-palmitoylethanolamine (PEA) (d), *N*-oleoylethanolamine (OEA) (e) and anandamide (AEA) (f) in human colon cancer tissues ($n = 8$) and adjacent non-tumour colon specimens ($n = 8$) ($n = 1$ outlier has been removed by ROUT test). The levels of NAEs are reported as pmol·mg$^{-1}$ of wet tissue weight. All the data are expressed as means ± SD; *$P < 0.05$ versus 'healthy', as assessed by paired Student's *t*-test; n.s., not significant

which is extensively used to study the mechanisms underlying human sporadic colon cancer as well as to evaluate drug potential chemo-preventive effects (Neufert et al., 2007). These results overall high-light for the first time the promising functional role of NAAA in CRC growth and development.

Nowadays, increasing interest is being paid to the analysis of a *repertoire* of proteins, termed 'secretome', released in the extracellular space by tumoural and stromal cells (Xue et al., 2008). This *reservoir* of secreted extracellular proteins includes growth factors, proteinases, immunoregulatory cytokines, cell motility factors or other bioactive molecules able to crucially regulate the tumour micro-environment and to sustain key tumoural processes including proliferation (Xue et al., 2008). In line with this notion, in this study, the secretome col-lected from CRC xenograft tumours induced down-regulation of NAAA expression in CRC cells. Furthermore, tumour secretomes from AM9053-treated tumour-bearing mice exhibited a marked reduction in the expression of EGF family members, which play a major role in regulating tumour cell proliferation (Yarden & Sliwkowski, 2001).

These findings, taken together, highlight the role of NAAA in CRC tumour proliferation and uncover novel potential mechanistic aspects of NAAA inhibition. Here, we did not identify the main components of the tumour secretome that are accountable for the observed effects of pharmacological NAAA inhibition. This aspect is of primary importance and deserves to be fully evaluated in the future.

In light of the in vivo results obtained here, we also investigated the pharmacological activity of the NAAA inhibitor on in vitro CRC cell proliferation. In line with previous preliminary data in bladder cancer cells (Vago et al., 2017), AM9053 exerted antiproliferative effects in two different colon adenocarcinoma cell lines without altering the growth of healthy cells, indicating that NAAA is likely engaged only in tumour proliferation mechanisms. In order to further explore the mechanism of actions involved in NAAA inhibition, we conducted pharmacological studies, in which selective antagonists (Alexander, Christopoulos, et al., 2021; Alexander, Cidlowski, et al., 2021; Alexander, Mathie, et al., 2021) of receptors (i.e. PPAR-α, TRPV1 and CB receptors) that are known to be targeted by the three main NAAA substrates (i.e. PEA, OEA and anandamide) (Di Marzo & Piscitelli, 2015) were incubated together with AM9053. Our results show that the antiproliferative effect of AM9053 in the CRC cells was decreased by PPAR-α or TRPV1 antagonists, suggesting that NAAA inhibition causes antiproliferative effects via elevation of NAEs and subsequent activation by these lipid mediators of two of their preferential molecular targets (i.e. AM9053 is acting as an indirect agonist on PPAR-α and TRPV1 receptors).

In order to further explore the antiproliferative effect of NAAA inhibition, we also investigated whether NAAA regulates cell cycle progression. We observed that NAAA inhibition affects colon cancer cell growth via S-phase cell cycle arrest, with a parallel decrease in the percentage of cells in the G0/G1 phase. This finding was further confirmed by the reduction of the expression of cyclin A2 and CDK2, two master inducers of the S phase (Heichman & Roberts, 1994).

In addition, we also observed that the NAAA inhibitor decreased migration rate of the two CRC cell lines with a different mechanism of action from the antiproliferative effects. Indeed, we found an involvement of PPAR-α and TRPV1 in proliferation, but not in migration. In any case, the involvement of NAAA in cell migration is in line with previous observations in bladder cancer cells (Vago et al., 2017).

To further confirm the involvement of NAAA in the antiproliferative action of AM9053, we induced the genetic silencing of the enzyme in the adenocarcinoma cell line HCT116. Notably, we found that siNAAA-HCT116 cells showed a reduced cell proliferation rate, thus confirming the phenotype observed using the pharmacological approach. Perhaps more importantly, AM9053 did not cause any effect in siNAAA-HCT116 cells, thus confirming the involvement of NAAA in AM9053 effects on CRC cell proliferation and the selectivity of the inhibitor for this enzyme at the concentration used. Importantly, siNAAA-HCT116 cells also exhibited the S-phase cell cycle arrest observed in AM9053-teated cells, with a parallel reduction in cyclin A2 expression.

NAAA expression has been previously associated with the aggressiveness of tumours, being inversely correlated with prostate cancer (Liu et al., 2014) and directly correlated with murine ovarian cancer (Du et al., 2016). Here, we have found that NAAA expression was strongly down-regulated in colonic biopsies of CRC patients in tumour tissue compared with the neighbouring healthy tissues. Whether or not changes in NAAA expression occur at early phases of tumour development (e.g. adenoma) has been not investigated in the present study. In line with the decrease in NAAA expression, we observed a strong augmentation of the three main NAAA substrates (PEA, OEA and anandamide) in CRC biopsies. Although the increase in anandamide levels has been previously documented (Ligresti et al., 2003), our study reports the first data about increased levels in CRC tissues of PEA and OEA, which are better substrates than anandamide for NAAA (Bottemanne et al., 2018). Indeed, we cannot exclude that the observed increased levels of anandamide might be due to mechanisms other than down-regulation of NAAA. One paper has reported that the levels of endocannabinoid-like lipids (i.e. PEA and OEA), as well as anandamide, were not altered in the blood samples of CRC patients (Grill et al., 2019). However, these results should be considered with caution because plasma levels of endocannabinoids and endocannabinoid-like mediators do not necessarily reflect colonic levels of these mediators and are also dependent on body mass index and HDL cholesterol levels (Cote et al., 2007).

The results on NAE levels in CRC tissues prompted us to take also into account the analysis of the expression of several targets belonging to the so-called endocannabinoidome system (Di Marzo & Piscitelli, 2015), including cannabinoid (CB$_1$ and CB$_2$) and non-cannabinoid (i.e. PPAR-α and TRPV1) receptors that are responsive to PEA, OEA and/or anandamide. We found here a significant down-regulation of CB receptors, which could represent an adaptive response to the increased levels of their endogenous ligands. This is not surprising because down-regulation of CB receptors has been already observed following chronic exposure to their endogenous ligands (Martini et al., 2007; Rajagopal & Shenoy, 2018). No changes have been registered in PPAR-α and TRPV1 expressions.

In conclusion, in this study we provide unprecedented evidence for the involvement of NAAA in CRC growth. Pharmacological NAAA inhibition by AM9053 caused a reduction of tumour growth and development in vivo as well as of tumour cell proliferation in vitro with a mechanism likely mediated by PPAR-α and TRPV1. Notably, AM9053 induced cell cycle arrest in the S phase possibly through cyclin A2/ CDK2 down-regulation. NAAA knock-down mirrored the effects of NAAA pharmacological inhibition. NAAA was down-regulated in human CRC tissues with subsequent increase in the tissue concentrations of its substrates (i.e. PEA, OEA and anandamide), which may represent an adaptive mechanism aiming at reducing CRC expansion. From a translational perspective, our discovery raises the interesting possibility that NAAA inhibitors may represent potential new drugs able to attenuate clinically diagnosed CRC growth and development. Specifically, AM9053, given its effect on a number of features of carcinogenesis shown here, may be considered for possible clinical evaluation in human CRC, if minimal toxicity in humans will be demonstrated.

## AUTHOR CONTRIBUTIONS

B.R., F.B. and A.A.I. are responsible for the conceptualization, activity planning and execution of the research and provided research funding. B.R. performed the experiments, collected and analysed the data and wrote the original draft of the paper. E.P. performed the in vivo experiments and collected and analysed the data of the manuscript. F.A.I. performed the RT-PCR on human and xenograft tissues. V.B. acquired the FACS data. F.P. performed the LC–MS. G.L., M.F.N., F.F., R.S., G.V., F.D.T., D.C., R.C. and T.V. helped in performing the in vitro and in vivo experiments. A.M. and M.M. developed and provided the AM9053. R.L., M.D.L., G.A. and M.D. provided the human tissues and relative cancer staging. B.S. helped in analysing the GENT2 data. V.D.M. helped in interpreting the data. A.A.I., V.D.M., F.B. and B.R. wrote the final version of the paper. All the authors approved the final version of the manuscript.

## CONFLICT OF INTEREST

The authors declare no conflicts of interest.

## DECLARATION OF TRANSPARENCY AND SCIENTIFIC RIGOUR

This Declaration acknowledges that this paper adheres to the principles for transparent reporting and scientific rigour of preclinical research as stated in the *BJP* guidelines for Design & Analysis, Immunoblotting and Immunochemistry and Animal Experimentation and as recommended by funding agencies, publishers and other organizations engaged with supporting research.

## DATA AVAILABILITY STATEMENT

The data that support the findings of this study are available from the corresponding author upon reasonable request.

## ORCID

*Barbara Romano* https://orcid.org/0000-0003-2772-5231
*Ester Pagano* https://orcid.org/0000-0003-2872-1734
*Fabio A. Iannotti* https://orcid.org/0000-0003-4480-8370
*Fabiana Piscitelli* https://orcid.org/0000-0001-9343-4622
*Vincenzo Brancaleone* https://orcid.org/0000-0002-0063-659X
*Giuseppe Lucariello* https://orcid.org/0000-0002-4593-2595
*Maria Francesca Nani* https://orcid.org/0000-0003-1462-3543
*Donatella Cicia* https://orcid.org/0000-0002-4054-0496
*Raffaele Capasso* https://orcid.org/0000-0002-3335-1822
*Tommaso Venneri* https://orcid.org/0000-0003-0195-2081
*Vincenzo Di Marzo* https://orcid.org/0000-0002-1490-3070
*Francesca Borrelli* https://orcid.org/0000-0002-2695-3294
*Angelo A. Izzo* https://orcid.org/0000-0002-8557-2133

## REFERENCES

Alexander, S. P., Christopoulos, A., Davenport, A. P., Kelly, E., Mathie, A., Peters, J. A., Veale, E. L., Armstrong, J. F., Faccenda, E., Harding, S. D., Pawson, A. J., Southan, C., Davies, J. A., Abbracchio, M. P., Alexander, W., Al-Hosaini, K., Bäck, M., Barnes, N. M., Bathgate, R., et al. (2021). The Concise Guide to PHARMACOLOGY 2021/22: G protein-coupled receptors. *British Journal of Pharmacology*, *178*(Suppl 1), S27–S156.

Alexander, S. P., Cidlowski, J. A., Kelly, E., Mathie, A., Peters, J. A., Veale, E. L., Veale, E. L., Armstrong, J. F., Faccenda, E., Harding, S. D., Pawson, A. J., Southan, C., Davies, J. A., Coons, L., Fuller, P. J., Korach, K. S., & Young, M. J. (2021). The Concise Guide to PHARMACOLOGY 2021/22: Nuclear hormone receptors. *British Journal of Pharmacology*, *178*(Suppl 1), S246–S263.

Alexander, S. P., Kelly, E., Mathie, A., Peters, J. A., Veale, E. L., Armstrong, J. F., Faccenda, E., Harding, S. D., Pawson, A. J., Southan, C., Buneman, O. P., Cidlowski, J. A., Christopoulos, A., Davenport, A. P., Fabbro, D., Spedding, M., Striessnig, J., Davies, J. A., Ahlers-Dannen, K. E., ... Zolghadri, Y. (2021). The Concise Guide to PHARMACOLOGY 2021/22: Introduction and other protein targets. *British Journal of Pharmacology*, *178*(Suppl 1), S1–S26.

Alexander, S. P., Mathie, A., Peters, J. A., Veale, E. L., Striessnig, J., Kelly, E., Armstrong, J. F., Faccenda, E., Harding, S. D., Pawson, A. J., Southan, C., Davies, J. A., Aldrich, R. W., Attali, B., Baggetta, A. M., Becirovic, E., Biel, M., Bill, R. M., & Catterall, W. A. (2021). The Concise Guide to PHARMACOLOGY 2021/22: Ion channels. *British Journal of Pharmacology*, *178*(Suppl 1), S157–S245.

Alexander, S. P. H., Roberts, R. E., Broughton, B. R. S., Sobey, C. G., George, C. H., Stanford, S. C., Cirino, G., Docherty, J. R., Giembycz, M. A., Hoyer, D., Insel, P. A., Izzo, A. A., Ji, Y., MacEwan, D. J., Mangum, J., Wonnacott, S., & Ahluwalia, A. (2018). Goals and practicalities of immunoblotting and immunohistochemistry: A guide for submission to the British Journal of Pharmacology. *British Journal of Pharmacology*, *175*, 407–411. https://doi.org/10.1111/bph.14112

Alhouayek, M., Bottemanne, P., Makriyannis, A., & Muccioli, G. G. (2017). *N*-acylethanolamine-hydrolyzing acid amidase and fatty acid amide hydrolase inhibition differentially affect *N*-acylethanolamine levels and macrophage activation. *Biochimica et Biophysica Acta Molecular and Cell Biology of Lipids*, *1862*, 474–484. https://doi.org/10.1016/j.bbalip.2017.01.001

Alhouayek, M., Bottemanne, P., Subramanian, K. V., Lambert, D. M., Makriyannis, A., Cani, P. D., & Muccioli, G. G. (2015). *N*-Acylethanolamine-hydrolyzing acid amidase inhibition increases colon *N*-palmitoylethanolamine levels and counteracts murine colitis. *FASEB Journal: Official Publication of the Federation of American Societies for Experimental Biology*, *29*, 650–661. https://doi.org/10.1096/fj.14-255208

Borrelli, F., Romano, B., Petrosino, S., Pagano, E., Capasso, R., Coppola, D., Battista, G., Orlando, P., Di Marzo, V., & Izzo, A. A. (2015). Palmitoylethanolamide, a naturally occurring lipid, is an orally effective intestinal anti-inflammatory agent. *British Journal of Pharmacology*, *172*, 142–158. https://doi.org/10.1111/bph.12907

Bottemanne, P., Muccioli, G. G., & Alhouayek, M. (2018). *N*-acylethanolamine hydrolyzing acid amidase inhibition: Tools and potential therapeutic opportunities. *Drug Discovery Today*, 23, 1520–1529. https://doi.org/10.1016/j.drudis.2018.03.007

Cote, M., Matias, I., Lemieux, I., Petrosino, S., Almeras, N., Despres, J. P., & Di Marzo, V. (2007). Circulating endocannabinoid levels, abdominal adiposity and related cardiometabolic risk factors in obese men. *International Journal of Obesity*, 31, 692–699. https://doi.org/10.1038/sj.ijo.0803539

Curtis, M. J., Alexander, S., Cirino, G., Docherty, J. R., George, C. H., Giembycz, M. A., Hoyer, D., Insel, P. A., Izzo, A. A., Ji, Y., MacEwan, D. J., Sobey, C. G., Stanford, S. C., Teixeira, M. M., Wonnacott, S., & Ahluwalia, A. (2018). Experimental design and analysis and their reporting II: Updated and simplified guidance for authors and peer reviewers. *British Journal of Pharmacology*, 175, 987–993. https://doi.org/10.1111/bph.14153

Di Marzo, V., & Piscitelli, F. (2015). The endocannabinoid system and its modulation by phytocannabinoids. *Neurotherapeutics*, 12, 692–698. https://doi.org/10.1007/s13311-015-0374-6

Du, F., Li, Y., Zhang, W., Kale, S. P., McFerrin, H., Davenport, I., Wang, G., Skripnikova, E., Li, X. L., Bowen, N. J., McDaniels, L. B., Meng, Y. X., Polk, P., Liu, Y. Y., & Zhang, Q. J. (2016). Highly and moderately aggressive mouse ovarian cancer cell lines exhibit differential gene expression. *Tumour Biology: The Journal of the International Society for Oncodevelopmental Biology and Medicine*, 37, 11147–11162. https://doi.org/10.1007/s13277-015-4518-4

Edge, S. B., & Compton, C. C. (2010). The American Joint Committee on Cancer: The 7th edition of the AJCC cancer staging manual and the future of TNM. *Annals of Surgical Oncology*, 17, 1471–1474. https://doi.org/10.1245/s10434-010-0985-4

Gerdes, J., Lemke, H., Baisch, H., Wacker, H. H., Schwab, U., & Stein, H. (1984). Cell cycle analysis of a cell proliferation-associated human nuclear antigen defined by the monoclonal antibody Ki-67. *Journal of Immunology*, 133, 1710–1715.

Grill, M., Hogenauer, C., Blesl, A., Haybaeck, J., Golob-Schwarzl, N., Ferreiros, N., Thomas, D., Gurke, R., Trötzmüller, M., Köfeler, H. C., Gallé, B., & Schicho, R. (2019). Members of the endocannabinoid system are distinctly regulated in inflammatory bowel disease and colorectal cancer. *Scientific Reports*, 9, 2358. https://doi.org/10.1038/s41598-019-38865-4

Heichman, K. A., & Roberts, J. M. (1994). Rules to replicate by. *Cell*, 79, 557–562. https://doi.org/10.1016/0092-8674(94)90541-X

Iannotti, F. A., Pagano, E., Guardiola, O., Adinolfi, S., Saccone, V., Consalvi, S., Piscitelli, F., Gazzerro, E., Busetto, G., Carrella, D., Capasso, R., Puri, P. L., Minchiotti, G., & Di Marzo, V. (2018). Genetic and pharmacological regulation of the endocannabinoid CB1 receptor in Duchenne muscular dystrophy. *Nature Communications*, 9, 3950. https://doi.org/10.1038/s41467-018-06267-1

Izzo, A. A., Aviello, G., Petrosino, S., Orlando, P., Marsicano, G., Lutz, B., Borrelli, F., Capasso, R., Nigam, S., Capasso, F., Di Marzo, V., & Endocannabinoid Research Group. (2008). Increased endocannabinoid levels reduce the development of precancerous lesions in the mouse colon. *Journal of Molecular Medicine (Berlin, Germany)*, 86, 89–98. https://doi.org/10.1007/s00109-007-0248-4

Kalyan, A., Kircher, S., Shah, H., Mulcahy, M., & Benson, A. (2018). Updates on immunotherapy for colorectal cancer. *Journal of Gastrointestinal Oncology*, 9, 160–169. https://doi.org/10.21037/jgo.2018.01.17

Ligresti, A., Bisogno, T., Matias, I., De Petrocellis, L., Cascio, M. G., Cosenza, V., D'argenio, G., Scaglione, G., Bifulco, M., Sorrentini, I., & Di Marzo, V. (2003). Possible endocannabinoid control of colorectal cancer growth. *Gastroenterology*, 125, 677–687. https://doi.org/10.1016/S0016-5085(03)00881-3

Lilley, E., Stanford, S. C., Kendall, D. E., Alexander, S. P. H., Cirino, G., Docherty, J. R., George, C. H., Insel, P. A., Izzo, A. A., Ji, Y., Panettieri, R. A., Sobey, C. G., Stefanska, B.,

Stephens, G., Teixeira, M., & Ahluwalia, A. (2020). ARRIVE 2.0 and the British Journal of Pharmacology: Updated guidance for 2020. *British Journal of Pharmacology*, 177, 3611–3616. https://doi.org/10.1111/bph.15178

Liu, Y., Chen, J., Sethi, A., Li, Q. K., Chen, L., Collins, B., Gillet, L. C. J., Wollscheid, B., Zhang, H., & Aebersold, R. (2014). Glycoproteomic analysis of prostate cancer tissues by SWATH mass spectrometry discovers *N*-acylethanolamine acid amidase and protein tyrosine kinase 7 as signatures for tumor aggressiveness. *Molecular & Cellular Proteomics: MCP*, 13, 1753–1768. https://doi.org/10.1074/mcp.M114.038273

Malamas, M., Makriyannis, A., Subramian, K. V. & Whitten, K. M. (2015). N-Acylethanolamine Hydrolyzing Acid Amidase (NAAA) inhibitors and their use thereof. WO2015179190A1.

Malvezzi, M., Carioli, G., Bertuccio, P., Boffetta, P., Levi, F., La Vecchia, C., & Negri, E. (2019). European cancer mortality predictions for the year 2019 with focus on breast cancer. *Annals of Oncology: Official Journal of the European Society for Medical Oncology*, 30, 781–787. https://doi.org/10.1093/annonc/mdz051

Martini, L., Waldhoer, M., Pusch, M., Kharazia, V., Fong, J., Lee, J. H., Freissmuth, C., & Whistler, J. L. (2007). Ligand-induced down-regulation of the cannabinoid 1 receptor is mediated by the G-protein-coupled receptor-associated sorting protein GASP1. *The FASEB Journal*, 21, 802–811. https://doi.org/10.1096/fj.06-7132com

Neufert, C., Becker, C., & Neurath, M. F. (2007). An inducible mouse model of colon carcinogenesis for the analysis of sporadic and inflammation-driven tumor progression. *Nature Protocols*, 2, 1998–2004. https://doi.org/10.1038/nprot.2007.279

Park, S. J., Yoon, B. H., Kim, S. K., & Kim, S. Y. (2019). GENT2: An updated gene expression database for normal and tumor tissues. *BMC Medical Genomics*, 12, 101. https://doi.org/10.1186/s12920-019-0514-7

Percie du Sert, N., Hurst, V., Ahluwalia, A., Alam, S., Avey, M. T., Baker, M., Browne, W. J., Clark, A., Cuthill, I. C., Dirnagl, U., Emerson, M., Garner, P., Holgate, S. T., Howells, D. W., Karp, N. A., Lazic, S. E., Lidster, K., MacCallum, C. J., Macleod, M., … Würbel, H. (2020). The ARRIVE guidelines 2.0: Updated guidelines for reporting animal research. *British Journal of Pharmacology*, 177, 3617–3624. https://doi.org/10.1111/bph.15193

Pisanti, S., Picardi, P., D'Alessandro, A., Laezza, C., & Bifulco, M. (2013). The endocannabinoid signaling system in cancer. *Trends in Pharmacological Sciences*, 34, 273–282. https://doi.org/10.1016/j.tips.2013.03.003

Rajagopal, S., & Shenoy, S. K. (2018). GPCR desensitization: Acute and prolonged phases. *Cellular Signalling*, 41, 9–16. https://doi.org/10.1016/j.cellsig.2017.01.024

Romano, B., Borrelli, F., Pagano, E., Cascio, M. G., Pertwee, R. G., & Izzo, A. A. (2014). Inhibition of colon carcinogenesis by a standardized *Cannabis sativa* extract with high content of cannabidiol. *Phytomedicine*, 21, 631–639. https://doi.org/10.1016/j.phymed.2013.11.006

Romano, B., Elangovan, S., Erreni, M., Sala, E., Petti, L., Kunderfranco, P., Massimino, L., Restelli, S., Sinha, S., Lucchetti, D., Anselmo, A., Colombo, F. S., Stravalaci, M., Arena, V., D'Alessio, S., Ungaro, F., Inforzato, A., Izzo, A. A., Sgambato, A., … Vetrano, S. (2019). TNF-stimulated gene-6 is a key regulator in switching stemness and biological properties of mesenchymal stem cells. *Stem Cells*, 37, 973–987. https://doi.org/10.1002/stem.3010

Sakura, Y., Tsuboi, K., Uyama, T., Zhang, X., Taoka, R., Sugimoto, M., Kakehi, Y., & Ueda, N. (2016). A quantitative study on splice variants of *N*-acylethanolamine acid amidase in human prostate cancer cells and other cells. *Biochimica et Biophysica Acta*, 1861, 1951–1958. https://doi.org/10.1016/j.bbalip.2016.09.018

Siegel, R. L., Miller, K. D., Fuchs, H. E., & Jemal, A. (2021). Cancer statistics, 2021. *CA: A Cancer Journal for Clinicians*, 71, 7–33. https://doi.org/10.3322/caac.21654

Su, A. I., Wiltshire, T., Batalov, S., Lapp, H., Ching, K. A., Block, D., Zhang, J., Soden, R., Hayakawa, M., Kreiman, G., Cooke, M. P., Walker, J. R., & Hogenesch, J. B. (2004). A gene atlas of the mouse and human protein-encoding transcriptomes. *Proceedings of the National Academy of Sciences of the United States of America*, *101*, 6062–6067. https://doi.org/10.1073/pnas.0400782101

Tsuboi, K., Sun, Y. X., Okamoto, Y., Araki, N., Tonai, T., & Ueda, N. (2005). Molecular characterization of *N*-acylethanolamine-hydrolyzing acid amidase, a novel member of the choloylglycine hydrolase family with structural and functional similarity to acid ceramidase. *The Journal of Biological Chemistry*, *280*, 11082–11092. https://doi.org/10.1074/jbc.M413473200

Tsuboi, K., Zhao, L. Y., Okamoto, Y., Araki, N., Ueno, M., Sakamoto, H., & Ueda, N. (2007). Predominant expression of lysosomal *N*-acylethanolamine-hydrolyzing acid amidase in macrophages revealed by immunochemical studies. *Biochimica et Biophysica Acta*, *1771*, 623–632. https://doi.org/10.1016/j.bbalip.2007.03.005

Vago, R., Bettiga, A., Salonia, A., Ciuffreda, P., & Ottria, R. (2017). Development of new inhibitors for *N*-acylethanolamine-hydrolyzing acid amidase as promising tool against bladder cancer. *Bioorganic & Medicinal Chemistry*, *25*, 1242–1249. https://doi.org/10.1016/j.bmc.2016.12.042

Wang, J., Zhao, L. Y., Uyama, T., Tsuboi, K., Wu, X. X., Kakehi, Y., & Ueda, N. (2008). Expression and secretion of *N*-acylethanolamine-hydrolysing acid amidase in human prostate cancer cells. *Journal of Biochemistry*, *144*, 685–690. https://doi.org/10.1093/jb/mvn122

West, J. M., Zvonok, N., Whitten, K. M., Vadivel, S. K., Bowman, A. L., & Makriyannis, A. (2012). Biochemical and mass spectrometric characterization of human *N*-acylethanolamine-hydrolyzing acid amidase inhibition. *PLoS ONE*, *7*, e43877. https://doi.org/10.1371/journal.pone.0043877

Xue, H., Lu, B., & Lai, M. (2008). The cancer secretome: A reservoir of biomarkers. *Journal of Translational Medicine*, *6*, 52. https://doi.org/10.1186/1479-5876-6-52

Yarden, Y., & Sliwkowski, M. X. (2001). Untangling the ErbB signalling network. *Nature Reviews Molecular Cell Biology*, *2*, 127–137. https://doi.org/10.1038/35052073

## SUPPORTING INFORMATION

Additional supporting information may be found in the online version of the article at the publisher's website.

**How to cite this article:** Romano, B., Pagano, E., Iannotti, F. A., Piscitelli, F., Brancaleone, V., Lucariello, G., Nanì, M. F., Fiorino, F., Sparaco, R., Vanacore, G., Di Tella, F., Cicia, D., Lionetti, R., Makriyannis, A., Malamas, M., De Luca, M., Aprea, G., D'Armiento, M., Capasso, R., Sbarro, B., Venneri, T., Di Marzo, V., Borrelli, F., & Izzo, A. A. (2022). *N*-Acylethanolamine acid amidase (NAAA) is dysregulated in colorectal cancer patients and its inhibition reduces experimental cancer growth. *British Journal of Pharmacology*, *179*(8), 1679–1694. https://doi.org/10.1111/bph.15737